

## Dissimilar welding of nickel-based Alloy 690 to SUS 304L with Ti addition

H.T. Lee <sup>a,\*</sup>, S.L. Jeng <sup>a</sup>, C.H. Yen <sup>a</sup>, T.Y. Kuo <sup>b,1</sup>

<sup>a</sup> Department of Mechanical Engineering, National Cheng Kung University, Tainan 701, Taiwan, ROC

<sup>b</sup> Department of Mechanical Engineering, Southern Taiwan University of Technology, Tainan 710, Taiwan, ROC

Received 28 August 2003; accepted 1 June 2004

### Abstract

This study investigates the effects of Ti addition on the weldability, microstructure and mechanical properties of a dissimilar weldment of Alloy 690 and SUS 304L. Shielding metal arc welding (SMAW) is employed to butt-weld two plates with three welding layers, where each layer is deposited in a single pass. To investigate the effects of Ti addition, the flux coatings of the electrodes used in the welding process are modified by varying additions of either a Ti–Fe compound or a Ti powder. The results indicate that the microstructure of the fusion zone (FZ) is primarily dendritic. With increasing Ti content, it is noted that the microstructure changes from a columnar dendritic to an equiaxed dendritic, in which the primary dendrite arm spacing (PDAS) becomes shorter. Furthermore, it is observed that the amount of Al–Ti oxide phase increases in the inter-dendritic region, while the amount of Nb-rich phase decreases. Moreover, the average hardness of the FZ increases slightly. The results indicate that Ti addition prompts a significant increase in the elongation of the weldment (i.e. 36.5%, Ti: 0.41 wt%), although the tensile strength remains relatively unchanged. However, at an increased Ti content of 0.91 wt%, an obvious reduction in the tensile strength is noted, which can be attributed to a general reduction in the weldability of the joint.

© 2004 Elsevier B.V. All rights reserved.

### 1. Introduction

In the past, there have been various instances where dissimilar weldments of Alloy 600 and SUS 308 Stainless Steel (SS) employed in nuclear power plant components have failed. These failures have generally been attributed to an inappropriate matching of the welded materials

and to an improper slot in the weldments [1]. Accordingly, researchers have attempted to identify a more robust combination of materials for dissimilar weldments. This study investigates the feasibility of replacing Alloy 600 and SUS 308 SS with Alloy 690 and SUS 304L SS, respectively. Although the latter materials are both Ni–Cr–Fe alloys, they exhibit significantly different material properties and vary greatly in cost since their Ni, Cr and Fe contents are very different. Alloy 690 is expensive, but has the advantage of excellent resistance to stress corrosion cracking (SCC) and inter-granular stress corrosion cracking (IGSCC). SUS 304L SS is a less expensive material and has found widespread application within general corrosion environments.

\* Corresponding author. Tel.: +886 6 275 7575x62154; fax: +886 6 274 5698.

E-mail addresses: [hlee@mail.ncku.edu.tw](mailto:hlee@mail.ncku.edu.tw) (H.T. Lee), [tykuo@mail.stut.edu.tw](mailto:tykuo@mail.stut.edu.tw) (T.Y. Kuo).

<sup>1</sup> Tel.: +886 6 253 3131x3511; fax: +886 6 253 7912.

In elevated temperature environments, Alloy 690 has a superior corrosion resistance due to its high Cr content (30 wt%) [2,3]. The application of an appropriate heat treatment can enhance its corrosion resistance even further. Consequently, this alloy is widely used to replace nuclear power plant components such as steam generator tubes, which were previously made of Alloy 600 [4–6]. SUS 304L SS is also employed within nuclear power plant components, e.g., for general components requiring corrosion resistance properties.

The mechanical and corrosion resistance properties of components are influenced not only by the base materials themselves, but also by the characteristics of the weld between them. This is particularly the case for dissimilar weldments. These weldments permit a reduction in the constructional cost of components [7], and consequently they continue to be the subject of considerable research. However, one problem associated with dissimilar weldments is that the obvious compositional variation and alloy transfer associated with the dilution of the two different base metals may result in failure of the weld [8]. The adoption of a filler metal compatible with both base metals has been proposed as a means of ameliorating this problem.

Inconel Filler Metal 82 (I-82), Inconel Welding Electrode 182 (I-182), Inconel Filler Metal 52 (I-52) and Inconel Welding Electrode 152 (I-152) are all suitable for the welding of Alloy 690. I-82 and I-182 were originally developed for the welding of Alloy 600, but are now also applied in the welding of Alloy 690. However, Page [6,9] indicated evidence of IGSCC in the resulting welds, and consequently, I-52 and I-152 were developed as alternative filler metals. A previous study has revealed a significant difference in the welding characteristics of these two filler metals, i.e., I-82 provides enhanced weldability and improved mechanical properties, whereas I-52 demonstrates superior corrosion resistance [10].

The Cr and Ni contents of a nickel-based alloy play an essential role in determining the corrosion resistance of the material. It has been shown previously that the IGSCC and SCC effects in a nickel-based alloy can be suppressed effectively by specifying either a 30 wt% Cr content or a 60 wt% Ni content [11]. Furthermore, both Cr and Ni have a high affinity with C and readily form carbides [12,13]. The heat generated during the welding process causes the Cr content to interact readily with the C to form carbides such as  $M_{23}C_6$  and  $M_7C_3$ , which then precipitate on the grain boundaries. This reaction may result in a Cr-depletion within the first-pass welding layer or in the heat affected zone (HAZ), which causes a degradation of the weldment's corrosion resistance. The problem of Cr-depletion can be avoided by either increasing the Cr and Ni content of the alloy, or by introducing high affinity elements such as Ti and Nb to stabilize the C [14].

Yamanaka et al. [15] have indicated that the addition of Nb in Alloy 600 is an effective means of enhancing its corrosion resistance properties. Furthermore, Lee and Kuo [16] demonstrated an improvement in the mechanical properties of Alloy 690 welds at room temperature through the addition of Nb. However, it has been shown by others that the resulting formation of an Nb-rich phase decreases the corrosion resistance of the weld [16]. Accordingly, researchers have investigated the use of Ti addition to improve the mechanical properties of dissimilar weldments.

It has been determined that the addition of Ti can reduce porosity, lessen welding defects and increase the strength of the FZ [17]. Furthermore, an appropriate addition in the weld metals for steels increases the toughness properties of the weld and eliminates weld segregation [18,19]. Since the affinity of Ti to C is greater than the affinity of Cr to C, Ti forms MC-type carbides with C much faster than Cr will do, and therefore Ti addition yields a significant increase in the corrosion resistance and mechanical properties of the weld [12–14]. However, since Ti is a strong deoxidizer, it is not readily retainable in welds, and consequently has a negative influence upon the weldability [20–22].

The intention of the current study is to investigate the effects of various levels of Ti addition on the welding feasibility, FZ microstructure, and mechanical properties of a dissimilar Alloy 690 and SUS 304L SS weldment. Ti addition is realized by modifying the Ti content of the electrode flux coating with varying percentages of either a pure Ti powder or a Ti–Fe compound.

## 2. Experimental procedure

This study concerns dissimilar weldments of Alloy 690 and SUS 304L. The compositions of these two materials are presented in Table 1. The Alloy 690 was supplied by Sumitomo Metal Technology Ltd., and had been heat-treated at 1050 °C for 5 min and then quenched in water prior to delivery. Meanwhile, the purchased SUS 304L was heat treated in the laboratory at 1050 °C for 2 h and then allowed to cool in air. Samples of both materials were then prepared with dimensions of 80 × 70 × 6 mm (length × width × thickness).

The compositions of the electrodes prepared for the current investigation were based on the Inconel Welding Electrode 152 series. (Note that Inconel is the trademark of INCO Alloys International, West Virginia, USA.) Oxford filler metal 52 of diameter  $\phi = 3.2$  mm was chosen as the core wire. (Note that Oxford is the trademark of Oxford Alloys Inc. Louisiana, USA.) A series of welding electrodes were prepared by coating the core wire with a flux containing various additions of either a Ti powder or a Ti–Fe compound. The compositions of the individual experimental electrodes were analyzed

Table 1  
The composition of base metals and welding electrodes (wt%)

	Ni	Cr	Fe	Mn	Nb	Ti	Mo	C	Si	Cu	Al	S	P
Alloy 690	60.65	29.70	8.76	0.29	–	0.20	–	0.022	0.35	0.02	–	0.001	0.007
SUS 304L	8.00	18.00	Bal	2.00	–	–	–	0.030	1.00	–	–	0.003	0.045
Oxford Filler Metal 52	60.00	29.30	8.80	0.40	0.02	0.500	0.100	0.030	0.17	0.060	0.61	0.010	–
Inconel Welding Electrodes 152	52.80	30.00	10.40	3.42	1.87	0.112	0.071	0.032	0.42	<0.005	0.14	0.008	0.009
Without extra addition <sup>a</sup> S009	51.20	29.60	11.70	3.99	1.82	0.099	0.072	0.048	0.47	0.061	0.06	0.009	0.019
Ti–Fe compound <sup>b</sup>													
STF013	51.90	28.50	12.00	3.88	1.90	0.132	0.073	0.048	0.52	0.062	0.06	0.008	0.019
STF027	51.50	28.30	12.40	3.78	1.96	0.271	0.077	0.047	0.64	0.062	0.06	0.008	0.018
Ti-powder <sup>c</sup>													
ST017	53.50	26.82	11.86	3.96	1.82	0.176	–	0.039	0.61	–	0.06	0.004	0.013
ST041	53.00	26.92	11.83	3.94	1.92	0.410	–	0.040	0.78	–	0.05	0.003	0.013
ST091	53.17	27.01	12.64	3.61	1.45	0.910	0.057	0.050	0.93	0.010	0.05	–	–

<sup>a</sup> Without extra Ti addition in the flux, the Ti content comes from the filler metal.

<sup>b</sup> Adding Ti–Fe compound in the flux to change the Ti content.

<sup>c</sup> Adding Ti-powder in the flux to change the Ti content.

in accordance with AWS/ASME SFA A5.11 specifications, and the results are presented in Table 1. The electrodes are designated in terms of their Ti content, i.e., S009 electrodes are those without extra additives, while the ST and STF electrodes contain Ti powder and Ti–Fe compounds, respectively. Furthermore, the digits within the designation of each electrode refer to the Ti content. A bead on plate (BOP) welding test was performed using each electrode under identical welding parameters (i.e. 65 A, 21 V, straight positive, DCSP). The corresponding results are shown in Table 2.

Fig. 1 presents the experimental arrangement adopted for the welding process. The beveled test plates to be welded together were arranged to form an 80° V groove with a 3.2 mm root opening gap and a 1 mm root face. A ceramic backing strip was stuck beneath the weldment. Prior to welding, the experimental electrodes were dried thoroughly, and the surfaces of the base metals and clamps were cleaned with acetone. The two test plates were then butt-welded using the SMAW welding process. A total of three welding layers were utilized, with each layer being deposited in a single pass. The slag

and oxide were completely removed after the completion of each pass, and the inter-pass temperature was allowed to fall below 150 °C before the next pass was performed. The SMAW welding parameters for each pass of each electrode are presented in Table 3.

Samples for microstructural analysis were ground and polished mechanically, and were then etched electrolytically under six volts DC for 20–30 s in a reagent of 70 ml H<sub>3</sub>PO<sub>4</sub> + 30 ml H<sub>2</sub>O. Optical microscopy was used to observe the varied microstructure of the weld. A scanning electron microscope (SEM) equipped with an energy disperse X-ray spectrometer (EDS) was employed to analyze the microstructure.

Regarding the mechanical properties of each weld, the average hardness of the FZ was measured using a Vickers hardness tester with a load of 200 g, and tensile testing was performed with an MTS 810 universal tensile testing machine at room temperature and with a crosshead speed of 0.02 mm s<sup>-1</sup>. In accordance with ASTM-E8 specifications, the dimensions of the tensile test specimens were as shown in Fig. 2. The ruptured specimens were then observed fractographically under an SEM.

Table 2  
The effect of Ti–Fe compound and Ti powder on the bead on plate welding (welding parameters: 65 A, 21 V, DCSP)

Specimen no.	Spatter	Fluidity	Smoke	Deslag	Appearance	Arc stability
S009	○	○	○	△	○	○
STF013	○	△	△	△	△	○
STF027	○	△	△	△	△	△
ST017	×	△	×	×	△	△
ST041	×	×	×	×	△	×
ST091	×	×	×	×	×	×

○ good; △ bad; × very bad.

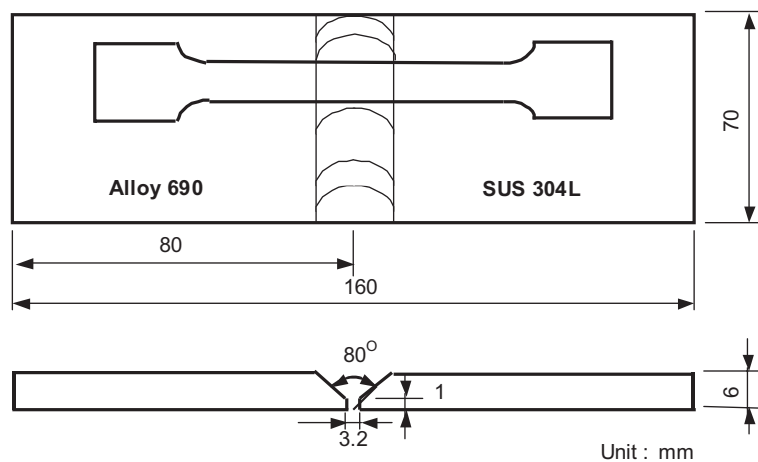
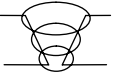


Fig. 1. The design of weldment.

Table 3  
Procedure and welding parameters for SMAW

Multi-pass schematic	Welding current	Specimen	Pass number	Welding parameters			Heat input ( $\text{kJ mm}^{-1}$ )	Total heat input ( $\text{kJ mm}^{-1}$ )	
				Current (A)	Voltage (V)	Welding speed ( $\text{mms}^{-1}$ )			
	DCSP	S009	3	65	21	1.43	0.72	2.05	
			2	65	21	1.55	0.66		
			1	100	22	2.45	0.67		
		STF013	3	65	21	1.18	0.87		2.41
			2	65	21	1.47	0.70		
			1	100	22	1.97	0.84		
		STF027	3	65	21	1.58	0.65		2.04
			2	65	21	1.73	0.59		
			1	100	22	2.07	0.80		
	AC	ST017	3	100	22	1.60	1.03	2.94	
			2	100	22	1.88	0.88		
			1	100	22	1.60	1.03		
		ST041	3	100	22	1.92	0.86	2.82	
			2	100	22	2.28	0.72		
			1	100	22	1.33	1.24		
ST091		3	100	22	2.17	0.76	3.02		
		2	100	22	2.52	0.65			
		1	100	22	1.02	1.61			

### 3. Results and discussion

#### 3.1. Weldability and weld composition

Table 2 shows the effects of Ti–Fe compound and Ti powder addition on the BOP welding process character-

istics under welding parameters of 65 A, 21 V, DCSP. It is observed that welding operation becomes more difficult as the Ti content increases. Under these conditions, thick smoke is generated during the welding process, particularly when welding is performed using electrodes with a Ti powder additive. It can be assumed that the

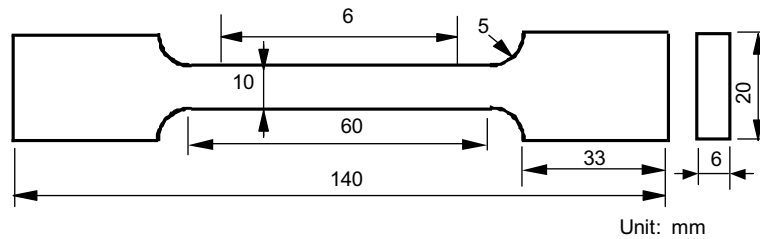


Fig. 2. The design of tensile test.

smoke formation is associated with the violent deoxidization of the Ti. Regarding the fluidity of the weld, the S009 electrode series provides the best results. As the Ti-powder addition increases, it is noted that the fluidity of molten metal, arc stability and deslag characteristics all deteriorate. It is also observed that the electrodes with a Ti–Fe compound additive yield less spatter than those with a Ti powder additive.

The results of Table 2 indicate that neither the addition of Ti powder nor the addition of Ti–Fe compounds enhances the fluidity of molten metal. It is noted that the S009 electrodes, which have the lowest Ti content, yield the best weldability results. Hence, it can be assumed that the severe oxidizing reaction of the Ti in the flux plays an important role here.

As stated above, the welding arc becomes more unstable as the level of Ti addition increases, especially in the case of electrodes containing a Ti-powder additive. Therefore, welding cannot be performed unless either the electrodes or the welding parameters are changed. Consequently, for the investigation of welds formed using the ST-series electrodes, the welding parameters were adjusted to 100 A, 22 V, AC, as shown in Table 3.

Fig. 3 presents the appearance of the welds produced with the six designed electrodes and their corresponding

welding parameters. It is observed that the welds with a Ti–Fe compound addition demonstrate a smooth and fine bead ripple due to the good fluidity of molten metal. However, the fluidity of those with a Ti powder additive deteriorates as the level of Ti content increases. Although the major composition (Ni, Cr, Fe) does not vary significantly, it is obvious that the weld appearance becomes rougher as the Ti content increases, especially for the case of the electrodes containing a Ti powder additive.

In this study, the transfer ratio of Ti from the additive of the electrodes to the welds is approximately 10%. Davis and Bailey [20] and Tanaka et al. [21] proposed that Mg and Al, which both react readily with oxygen, could reduce the loss of Ti through oxidation at high temperatures.

Additionally, the contents of Si and Fe rise as the level of Ti increases, regardless of whether the Ti addition is in the form of a Ti-powder or of a Ti–Fe compound. This phenomenon is attributed to the fact that Ti has a higher affinity to oxygen than either Si or Fe. Hence, their oxidization is reduced, and their contents increased accordingly. Furthermore, since the addition of Ti lowers the oxygen content in the weld, there is an appreciable improvement in the toughness of the weld [22].

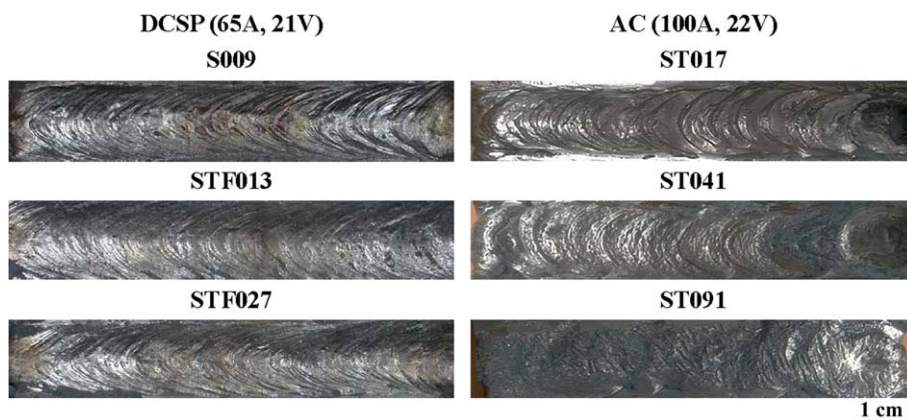


Fig. 3. The appearance of weld.

### 3.2. Microstructural analysis of fusion zone

Fig. 4 presents the macrostructure of the S009 weldment (without extra Ti addition). It can be seen that the resulting structure is mainly dendritic when the Ti content of the electrode is not modified. As shown in Fig. 5, when the level of Ti addition increases, the microstructure with Ti–Fe compound addition changes from a columnar dendritic and equiaxed dendritic structure to an equiaxed dendritic structure. However, as shown in Fig. 6, the FZ microstructure with Ti-powder addition does not change significantly, but remains predominantly with a columnar dendritic structure.

The PDAS of the various welds in their cap and root regions were measured. The corresponding results are shown in Fig. 7. It is clear that the PDAS in the welds with Ti–Fe compound addition is denser than in the welds with Ti-powder addition. This difference can be attributed to the different cooling rates (welding speeds), heat inputs (current  $\times$  voltage/welding speed), and Ti contents associated with the different electrodes.

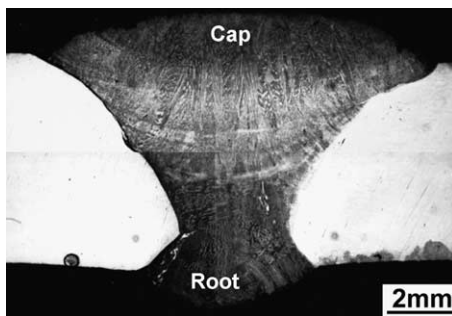


Fig. 4. The optical graph of S009 weldment.

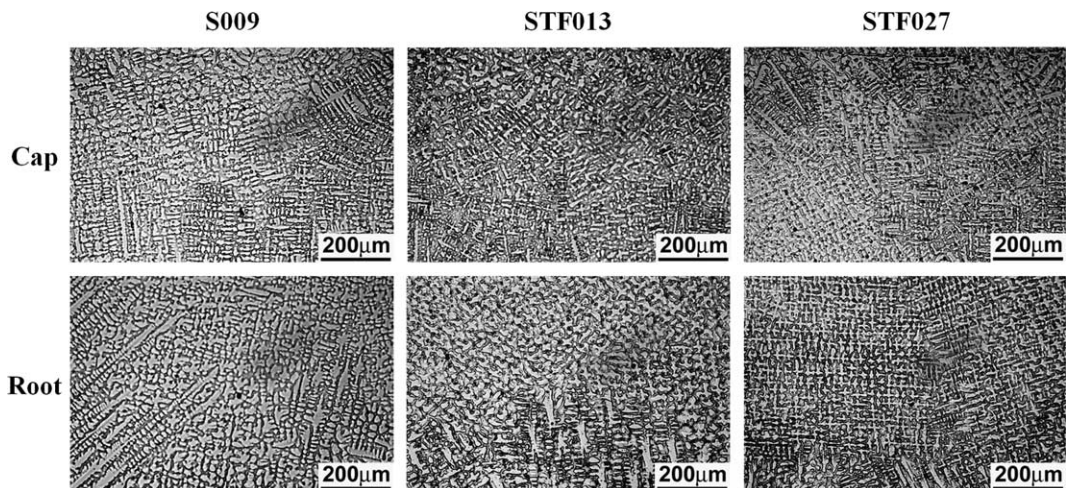


Fig. 5. The micrograph of the central fusion zone with the Ti–Fe compound additive (welding parameters: 65 A, 21 V, DCSP).

A faster welding speed results in a higher cooling rate and a lowered heat input, which tends to refine the PDAS [23]. According to Table 3, although the welding speeds of the STF-electrodes only exceeds that of ST-electrodes slightly, the heat input of STF-electrodes is much lower owing to a small current. Therefore, the PDAS in the STF welds will generally be finer than in the ST welds.

Compared to the cap layer (i.e. the third welding layer), the results reveal that the root has a shorter PDAS. This result is mainly attributed to the greater temperature gradient, which causes a faster cooling rate. When welding the first pass (the root), the base metals are at room temperature. However, the base metals are at a temperature of about 150 °C when welding the third pass (the cap). Consequently, the temperature gradient is relatively higher in the root. This induces a faster cooling rate and hence a more refined microstructure.

Additionally, Fig. 7 reveals that the PDAS decreases significantly in the ST-series electrodes as the addition of Ti increases. It is mainly contributed to the level of Ti addition. Thaulow's study has indicated the refinement of PDAS in the weld with the Ti addition [19]. This result arises from the occurrence of high constitutional cooling.

The increase in Ti addition causes a corresponding increase in inter-dendritic phases. These phases may be categorized as Nb-rich phases with an irregular slender shape in the low Ti-addition electrodes, as shown in Fig. 8(a), or as Al–Ti oxides and Al–Ti–Nb-rich particles with a spherical shape in the high Ti-addition electrodes, i.e., as shown in Fig. 8(b) and (c).

The Nb-rich phases evident in Fig. 8(a) are assumed to form in the later stages of the solidification process. At that time, the remaining inter-dendritic liquid is rich in solute atoms, including Nb, and Nb-rich phases tend

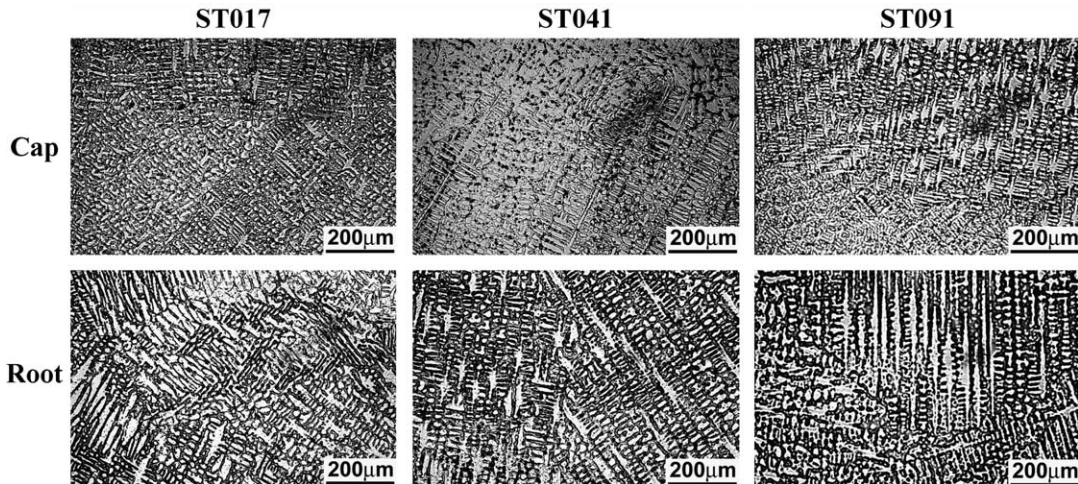


Fig. 6. The micrograph of the central fusion zone with the Ti powder additive (welding parameters: 100 A, 22 V, AC).

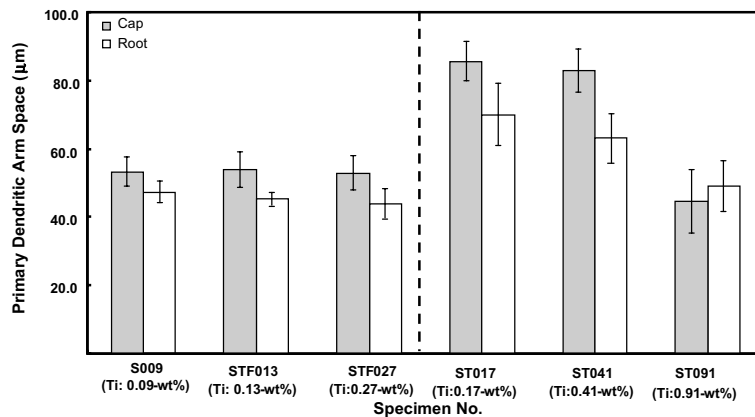


Fig. 7. The measurement of primary dendritic arm space (PDAS) in the central weld.

to form [16]. These phases are generally larger than the Al–Ti oxides. Additionally, as the level of Ti addition increases, these phases become smaller.

The Al–Ti–Nb-rich particles evident in Fig. 8(c) are assumed to be a mixture of Al–Ti oxides and Nb-rich phases since the affinity of Al and Ti to oxygen is higher than Nb. The usual intention of adding Al and Ti in the flux is to promote deoxidation in order to reduce porosity in the weld. In this case, most of the oxides would float to the surface of the welds to form part of the slag, while only a minority would remain within the weld in the form of spherical particles.

An observation of the inter-dendritic phase reveals that the Al–Ti oxides increase with higher levels of Ti content. Conversely, the Nb-rich phases decrease and become smaller. As a result of blending with the Al–Ti oxides, shown as Fig. 8(b), the size of the Nb-rich phases shrink,

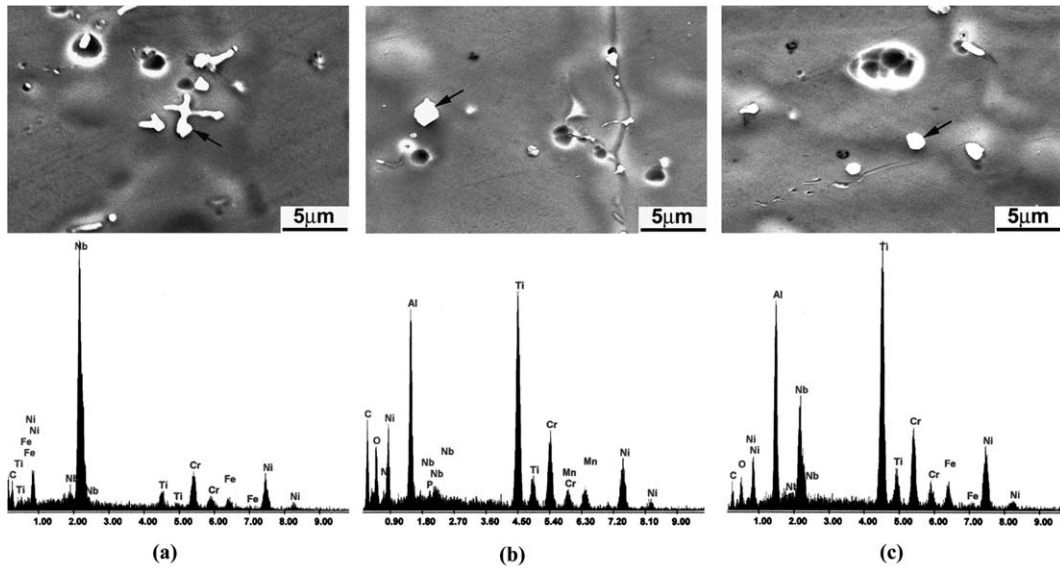
and consequently Nb-rich phases are less evident than Al–Ti–Nb-rich particles in the inter-dendritic region.

### 3.3. Mechanical property tests

#### 3.3.1. Hardness testing

Fig. 9 presents the results of hardness testing. It can be seen that the average hardness of the weld increases with increasing Ti content. In general, it is noted that the hardness in the root exceeds that in the cap. However, in the case of the ST091 electrode, which possesses the highest Ti content, the average hardness of the cap and root is similar.

The root is formed in the first welding pass of the welding process and the base metals are initially at room temperature. Therefore, this pass has a higher cooling rate than the third welding pass, i.e., the cap. Hence,



		C	O	Al	Nb	Ti	Cr	Fe	Ni
(a)	wt-%	12.86	-	-	56.12	3.10	10.09	2.98	14.85
	at-%	47.80	-	-	26.97	2.89	8.67	2.38	11.30
(b)	wt-%	11.01	15.10	15.67	2.74	23.44	12.52	-	16.34
	at-%	25.84	26.60	16.36	0.83	13.79	6.79	-	7.84
(c)	wt-%	3.21	6.02	15.20	14.89	26.77	11.44	4.33	18.14
	at-%	10.54	14.86	22.25	6.33	22.07	8.69	3.06	12.20

Fig. 8. The analysis of inter-dendritic phase: (a) Nb-rich phase in S009; (b) Al-Ti oxide in ST091; (c) Al-Ti-Nb-rich particles in ST091.

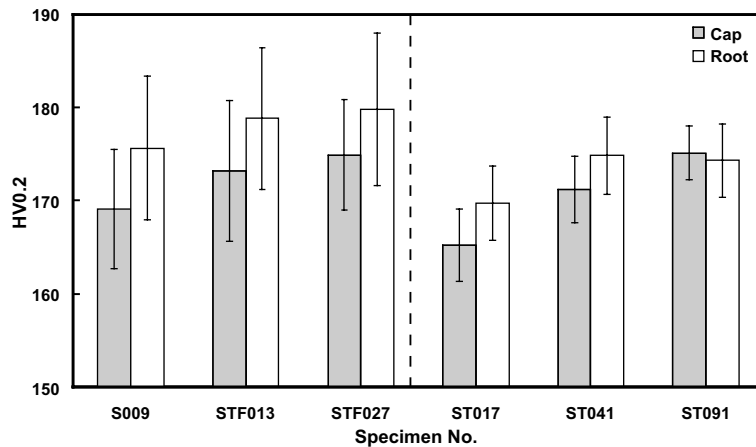


Fig. 9. The average hardness of fusion zone.

the dendrite structures within the root are correspondingly finer than those of the cap. It has been indicated that a higher cooling rate tends to enhance the hardness [16]. Consequently, the root has a higher hardness than the cap. Furthermore, since the total weld is achieved

using a multi-pass process, a greater degree of residual stress and deformation is induced within the root [24], and this also contributes to a higher average hardness.

As stated above, the average hardness in the cap and the root is approximately equal in the case of the ST091



electrode. It is assumed that this is the result of an increased occurrence of constitutional cooling due to the increase of Ti addition. Generally, a cap with a low dilution tends to have a relatively greater constitutional cooling. Therefore, a denser dendritic structure occurs in the cap due to the greater constitutional cooling.

The hardness testing results indicate that the average hardness of the welds produced using the Ti–Fe compound additive is higher than that of the welds formed using the Ti powder additive. This result is attributed to the larger current, which causes a greater heat input in the welds, when using the Ti-powder additive electrodes.

3.3.2. Tensile test

Fig. 10 presents the results of tensile testing. It is noted that each specimen ruptured within the FZ. Furthermore, it can be seen that an increased Ti content results in a greater elongation of the specimen prior to

rupture, but that the tensile strength remains approximately constant. Of the various specimens, the specimen produced using the high Ti electrode, i.e., ST091, is the first to fracture. This suggests that the poor weldability associated with a high Ti content (0.91 wt%) causes a general degradation of the weldment’s mechanical properties even though its average hardness is improved.

Fig. 11 presents images of the ductile rupture of each of the specimens. It is clear that the quantity of inter-dendritic phases in the rupture zone increases significantly as the level of Ti addition increases. It appears that holes are formed initially within the inter-dendritic phases, and that these holes gradually link with each other and result in the eventual rupturing of the specimen. When the shapes of the inter-dendritic phases are enhanced, the elongation of the specimen will be enhanced. However, when an increased number of irregular inter-dendritic phases are formed, the elongation will

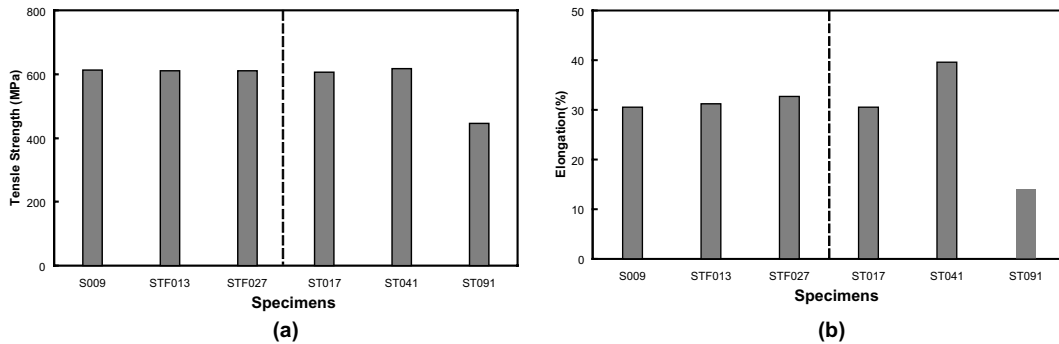


Fig. 10. The result of tensile test: (a) tensile strength and (b) elongation.

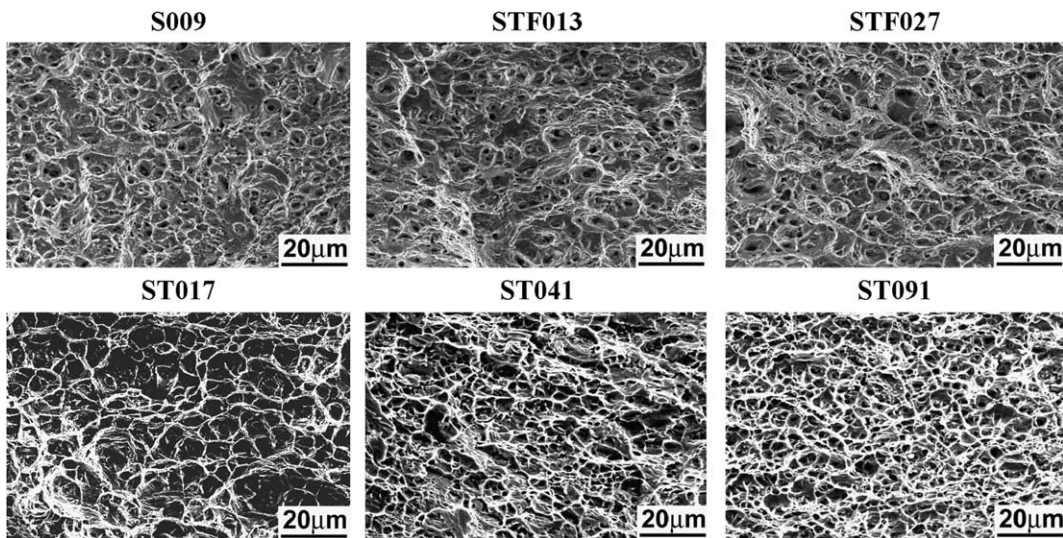


Fig. 11. The micrograph of root rupture.

decrease. These phases are particularly evident in the fracture of the low Ti addition specimen, S009, and explain the early rupture of this particular specimen and its reduced elongation.

In the case of ST091, a great number of inter-dendritic phases are induced in the weld. These phases generally have a spherical form. From the rupture results, it can be seen that the dimples on the ST091 surface are denser than those of the other specimens. Therefore, it is assumed that the poor weldability decreases the elongation and tensile strength of ST091.

It is also possible that large inter-dendritic phases could be a fundamental cause of the degradation of a weldment's mechanical properties. Previously, Lee et al. [25] stated that a higher Nb addition results in larger inter-dendritic phases, which prompt the weldment to rupture within the inter-dendritic region. The results of the present study suggest that an appropriate amount of Ti addition may cause a finer microstructure and smaller inter-dendritic phases, which increases the elongation of the weldment rather than lowering its strength under the conditions of high heat input.

#### 4. Conclusions

(1) It has been demonstrated that the electrodes with Ti powder addition generate more smoke, an unstable arc, a larger spark, and display a poorer welding operation than those with Ti–Fe compound addition. Additionally, it has been noted that the fluidity and deslag of the weld deteriorate as the level of Ti addition increases.

(2) The results have shown that a Ti–Fe compound additive is added, the microstructure tends to change from one of columnar dendrite to one of equiaxial dendrite as the level of Ti addition increases. Moreover, it has been noted that the PDAS shortens with increasing Ti content, particularly in the electrodes with a Ti-powder additive.

(3) Observations of the inter-dendritic phase have revealed the presence of irregular Nb-rich phases, Al–Ti oxides and Al–Ti–Nb-rich particle. It has been shown that the Al–Ti oxides tend to dominate in this region with increasing Ti addition.

(4) Hardness testing has revealed that the addition of Ti enhances the average hardness of the FZ. Because of the lower welding heat and the faster welding speed, the welds with a Ti–Fe compound additive have a higher hardness than those with a Ti-powder additive.

(5) Tensile testing has shown that all specimens fracture in the FZ and that the failure mode is one of ductile rupture. When the Ti content increases, it has been shown that the tensile strength remains constant, but that the elongation is considerably improved. However,

a Ti addition in excess of 0.91% will prompt the early failure of the specimen.

#### Acknowledgments

The authors gratefully acknowledge the financial support provided to this study by the National Science Council, Taiwan, under grant number: NSC 89-2216-E-006-065. The authors also wish to recognize the assistance provided by Tien-Tai Electrode Co. Ltd. Group in preparing the welding electrodes.

#### References

- [1] T. Ishihara, *Weld. J.* 68 (1989) 209s.
- [2] Inconel 690, Huntington Alloys, Huntington, WV, 1985, p. 1.
- [3] K. Stiller, J. Nilsson, K. Norring, *Metall. Trans. A* 27A (1996) 327.
- [4] G.J. Theus, R.H. Emanuelson, S.F. Chou, Stress corrosion cracking of Alloy 600 and 690 in all volatile treated water at elevated temperature, EPRI Report NP-3061 Palo Alto, CA, 1983, p. 1.
- [5] R.A. Page, A. McMinn, Stress corrosion cracking resistance of Alloys 600 and 690 and compatible weld metals in BWRs, EPRI Report NP-5882M, Palo Alto, CA, 1988, p. 1.
- [6] R.A. Page, *Corrosion* 39 (1983) 409.
- [7] H.T. Lee, S.L. Jeng, *Sci. Technol. Weld. Joining* 6 (2001) 225.
- [8] B.E. Payne, *Met. Constr.* 1 (1969) 79.
- [9] R.A. Page, Stress corrosion cracking of Alloy 600 and 690 and weld metals no. 82 and no.182 in high temperature water, EPRI Report NP-2617 Palo Alto, CA, 1982, p. 1.
- [10] H.T. Lee, T.Y. Kuo, *Sci. Technol. Weld. Joining* 4 (1999) 94.
- [11] H. Nagano, K. Yamanaka, K. Kobayashi, M. Inoue, *Sumitomo Search* 40 (1989) 57.
- [12] C.T. Sims, W.C. Hangel, *The Super Alloys*, John Wiley, New York, 1972, p. 145.
- [13] C.T. Sims, N.S. Stoloff, W.C. Hangel, *Super Alloys II*, John Wiley, New York, 1987, p. 111.
- [14] E. Folkhard, G. Rabensteiner, E. Perteneder, H. Schabreiter, J. Tösch, *Welding Metallurgy of Stainless Steels*, Springer-Verlag, New York, 1984, p. 112.
- [15] K. Yamanaka, K. Ogawa, K. Kobayashi, S. Nagata, *Sumitomo Search* 51 (1993) 15.
- [16] H.T. Lee, T.Y. Kuo, *Sci. Technol. Weld. Joining* 4 (1999) 246.
- [17] R.T. Holt, W. Wallace, *Int. Met. Rev.* 3 (1976) 24.
- [18] G.M. Evans, *Weld. J.* 75 (1996) 251s.
- [19] C. Thaulow, in: *International Conference on Welding Pool Chemistry and Metallurgy*, The Welding Institute, London, 15–17 April 1980, p. 17.
- [20] M.L.E. Davis, N. Bailey, in: *International Conference on Welding Pool Chemistry and Metallurgy*, The Welding Institute, London, 15–17 April 1980, p. 289.

- [21] J. Tanaka, T. Kitada, Y. Naganawa, Y. Kunisada, H. Nakagawa, in: International Conference on Welding Pool Chemistry and Metallurgy, The Welding Institute, London, 15–17 April 1980, p. 279.
- [22] S. Kou, *Welding Metallurgy*, Wiley, New York, 1987, p. 70.
- [23] S. Kou, *Welding Metallurgy*, Wiley, New York, 1987, p. 171.
- [24] I. Gowrisankar, A.K. Bhaduri, V. Seetharaman, D.D.N. Verma, D.R.G. Achar, *Weld. J.* 66 (1987) 147s.
- [25] H.T. Lee, S.L. Jeng, T.Y. Kuo, *Metal. Mater. Trans. A* 34A (2003) 1097.